

Synthetic triterpenoid 2-cyano-3,12-dioxooleana-1,9-dien-28-oic acid induces growth arrest in HER2-overexpressing breast cancer cells

Marina Konopleva,¹ Weiguo Zhang,¹ Yue-Xi Shi,¹ Teresa McQueen,¹ Twee Tsao,¹ Maen Abdelrahim,⁶ Mark F. Munsell,² Mary Johansen,³ Dihua Yu,⁴ Timothy Madden,³ Stephen H. Safe,⁶ Mien-Chie Hung,⁵ and Michael Andreeff¹

Section of Molecular Hematology and Therapy, Departments of ¹Blood and Marrow Transplantation, ²Biostatistics and Applied Mathematics, ³Experimental Therapeutics, ⁴Surgical Oncology, and ⁵Molecular and Cellular Oncology, The University of Texas M.D. Anderson Cancer Center; ⁶Institute for Biosciences and Technology, Texas A&M University Health Science Center, Houston, Texas

Abstract

HER2 overexpression is one of the most recognizable molecular alterations in breast tumors known to be associated with a poor prognosis. In the study described here, we explored the effect of HER2 overexpression on the sensitivity of breast cancer cells to the growth-inhibitory effects of 2-cyano-3,12-dioxooleana-1,9-dien-28-oic acid (CDDO), a synthetic triterpenoid, both *in vitro* and *in vivo* in a xenograft model of breast cancer. Both cell growth and colony formation in the soft agar assay, a hallmark of the transformation phenotype, were preferentially suppressed in HER2-overexpressing cell lines at low concentrations of CDDO, whereas growth-inhibitory effects at high concentrations did not correlate with the expression level of HER2. CDDO dose-dependently inhibited phosphorylation of HER2 in HER2-overexpressing cells and diminished HER2 kinase activity *in vitro*. CDDO induced the transactivation of the nuclear receptor peroxisome proliferator-activated receptor- γ in both vector control and HER2-transfected MCF7 cells. Dose-response

studies showed that the growth inhibition seen at lower concentrations of CDDO correlated with induction of the tumor suppressor gene caveolin-1, which is known to inhibit breast cancer cell growth. CDDO also reduced cyclin D1 mRNA and protein expression. *In vivo* studies with liposomally encapsulated CDDO showed complete abrogation of the growth of the highly tumorigenic MCF7/HER2 cells in a xenograft model of breast cancer. These findings provide the first *in vitro* and *in vivo* evidence that CDDO effectively inhibits HER2 tyrosine kinase activity and potently suppresses the growth of HER2-overexpressing breast cancer cells and suggest that CDDO has a therapeutic potential in advanced breast cancer. [Mol Cancer Ther 2006;5(2):317–28]

Introduction

One of the most common molecular alterations associated with the malignant phenotype of breast cancer is the overexpression of epidermal growth factor receptor-2 (also known as HER2). The HER2 receptor is the protein product of the *HER2* proto-oncogene and a member of the epidermal growth factor receptor family of transmembrane tyrosine kinases. Overexpression of HER2 can transform normal mammary epithelial cells and is amplified in 25% to 30% of breast cancers; it is associated with an aggressive form of the disease characterized by significantly shortened survival times (1).

Multiple lines of experimental evidence suggest that the overexpression of HER2 confers antiestrogen resistance on breast tumor cells (2). HER2 overexpression also confers resistance to paclitaxel (Taxol; ref. 3) and alkylating agents (cisplatin and cyclophosphamide; ref. 1). Trastuzumab, a recombinant monoclonal antibody against HER2, has shown some clinical benefit in HER2-overexpressing metastatic breast cancer. However, only a modest response to this highly selective inhibitor was seen when it was given as a single agent, with most cancers becoming resistant to the agent within <12 months of the start of therapy (4). Therefore, it is imperative to identify new agents that can arrest cell growth or induce apoptosis in HER2-overexpressing resistant breast cancer cells.

The novel triterpenoid 2-cyano-3,12-dioxooleana-1,9-dien-28-oic acid (CDDO) is effective in inducing apoptosis in leukemic (5–7), multiple myeloma (8, 9), lung cancer (10), ovarian cancer (11), osteosarcoma (12), and melanoma (13) cells. CDDO reportedly binds to and transactivates the nuclear receptor peroxisome proliferator-activated receptor γ (PPAR γ ; ref. 14), a transcription factor that controls key differentiation genes. PPAR γ ligands have been reported to inhibit the proliferation of malignant cells from different tissues, such as liposarcoma and breast, prostate, colon,

Received 8/31/05; revised 11/15/05; accepted 12/8/05.

Grant support: National Cancer Institute grants CA55164, CA16672, and CA49639 and the Paul and Mary Haas Chair in Genetics (M. Andreeff); National Institute of Environmental Health Sciences grant ES09106 (S.H. Safe); and Susan G. Komen Breast Cancer Foundation (M. Konopleva).

The costs of publication of this article were defrayed in part by the payment of page charges. This article must therefore be hereby marked advertisement in accordance with 18 U.S.C. Section 1734 solely to indicate this fact.

Note: M. Konopleva and W. Zhang contributed equally to this work.

Requests for reprints: Michael Andreeff, Department of Blood and Marrow Transplantation, The University of Texas M.D. Anderson Cancer Center, Unit 448, 1400 Holcombe Boulevard, Houston, TX 77030. Phone: 713-792-7260; Fax: 713-794-4747. E-mail: mandreeff@mdanderson.org

Copyright © 2006 American Association for Cancer Research.

doi:10.1158/1535-7163.MCT-05-0350

non-small cell lung, pancreatic, bladder, and gastric carcinoma cells (15, 16). This effect has been linked to the inhibition of G₀-G₁-S phase cell cycle progression, down-regulation of cyclin D1, enhanced expression of p21 or p27 cyclin-dependent kinase inhibitors, and induction of apoptosis. Activation of PPAR γ by 15-deoxy- Δ 12,14-prostaglandin J2 was also reported to dramatically inhibit HER2 tyrosine phosphorylation, which resulted in cell growth suppression and apoptosis (17). PPAR γ ligands also inhibit growth of PPAR γ -deficient cells (18), and PPAR γ -independent responses have been reported in several cancer cell lines (19–21).

We have shown previously that CDDO induces apoptosis in leukemic cells (22, 23) and inhibits the proliferation of both estrogen receptor (ER)-positive and ER-negative breast cancer cells (24) in part by activating PPAR γ signaling. However, CDDO inhibited growth of ovarian cancer cells irrespective of the PPAR γ status of the cells (11). In this study, we investigated the effects of CDDO on HER2-overexpressing breast cancer cells and the mechanisms of these responses. We observed that CDDO is capable of inhibiting growth of HER2-overexpressing cells, both *in vitro* and in a xenograft murine model of breast cancer, in part via the PPAR γ -dependent induction of caveolin-1 expression. These results indicate that CDDO may be useful as an adjunct or alternative therapy to conventional chemotherapy for chemoresistant breast cancer.

Materials and Methods

Chemicals, Antibodies, and Other Materials

CDDO was manufactured through the NIH Rapid Access to Interventional Development Program and kindly provided by Drs. E. Sausville (Developmental Therapeutics Program, Division of Cancer Treatment and Diagnosis, National Cancer Institute, Bethesda, MD) and M. Sporn (Department of Pharmacology, Dartmouth Medical School, Hanover, NH). A stock solution of 10 mmol/L CDDO in DMSO was kept stored at -20°C .

Proteasome inhibitors MG132 and proteasome inhibitor I were purchased from Calbiochem Co. (San Diego, CA). [γ -³²P]ATP and [³²P]dCTP were purchased from Amersham Pharmacia Biotech (Buckinghamshire, United Kingdom). Cyclin D1 and β_2 -microglobulin primers and probes were described by us previously (24). HER2 primers (forward 5'-CCTGCCAGTCCCGAGACCCACCT-3' and reverse 5'-TTGGTGGCAGGTAGGTGAGTT-3') were synthesized by Sigma Genosys (The Woodlands, TX). Glyceraldehyde-3-phosphate dehydrogenase probe was kindly provided by Dr. Duen-Hwa Yan (Department of Molecular and Cellular Oncology, The University of Texas M. D. Anderson Cancer Center, Houston, TX). Mouse monoclonal antibody HER2/ErbB2 and rabbit polyclonal antibody phospho-HER2 were from Cell Signaling Technology (Beverly, MA); cyclin D1 and cyclin E monoclonal antibodies from Calbiochem; mouse monoclonal antibody PPAR γ , rabbit polyclonal phosphotyrosine, and caveolin-1 antibodies were from Santa Cruz Biotechnology (Santa

Cruz, CA); and mouse monoclonal antibody ER- α was from DakoCytomation (Glostrup, Denmark). Terminal deoxynucleotide transferase-mediated dUTP nick end labeling (TUNEL) kit was purchased from Roche Diagnostics Corp. (Mannheim, Germany). All of the other chemicals and solvents were of the highest grade commercially available.

Cell Lines and Cell Culture

Breast cancer cell lines that express different levels of HER2, including stably transfected MCF7/HER2 and MDA-MB-435/HER2 cells and their vector controls (25) and SKBR3 cells that constitutively overexpress HER2 (a gift from Dr. Xiaofeng Le, Department of Experimental Therapeutics, The University of Texas M. D. Anderson Cancer Center), were used as *in vitro* model systems. The cells were cultured in DMEM/F12 supplemented with 10% (v/v) FCS and L-glutamine. Cells were maintained at 37°C in an atmosphere of 5% CO₂-95% air.

Growth Viability Assay

Effects of cell growth were assessed by using the 3-(4,5-dimethylthiazol-2-yl)-5-(3-carboxymethoxyphenyl)-2-(4-sulfophenyl)-2H-tetrazolium, inner salt assay (Promega, Madison, WI). This assay, a colorimetric method for determining the number of viable cells, is based on the bioreduction of 3-(4,5-dimethylthiazol-2-yl)-5-(3-carboxymethoxyphenyl)-2-(4-sulfophenyl)-2H-tetrazolium, inner salt by cells to a formazan product that is soluble in tissue culture medium and can be detected spectrophotometrically. MCF7/Neo, MCF7/HER2, MDA-MB-435/Neo, and MDA-MB-435/HER2 cells were plated in 96-well flat-bottomed plates (Corning, Inc., Corning, NY). The seeded number of cells was 2,000 per well, which was required to obtain an absorbance of ~ 1.0 to 1.5 at a wavelength of 490 nm, the linear range of the assay, after 72 hours of growth (determined empirically). After overnight incubation, cell culture media were replaced with freshly prepared DMEM/F12 containing 10% FCS and indicated concentrations of CDDO (1, 2.5, and 5 $\mu\text{mol/L}$) and DMSO for 72 hours of incubation. All experimental points were set up in six wells, and all experiments were repeated at least twice. The data were analyzed by ANOVA using Statistica version 6.1 (StatSoft, Inc., Tulsa, OK). IC₅₀s were generated based on the absorbance values using CalcuSyn version 1.2 (BioSoft, Inc., Ferguson, MO).

Colony Formation in Soft Agarose

Cells (1,000 per well) were seeded in 24-well plates in culture medium containing 0.35% low-melting agarose over a 0.7% agarose base layer in the presence of different concentrations of CDDO or vehicle and incubated for 14 days at 37°C in a humidified 95% O₂-5% CO₂ atmosphere in DMEM/F12 supplemented with 10% FCS and L-glutamine. Colonies were then stained with *p*-iodonitrotetrazolium violet (1 mg/mL stock diluted at 1:500) for 16 hours, and colonies larger than 100 μm in diameter were counted under the Leica stereofluorescence microscope MZFL III (Leica Microsystems, Dallas, TX). Each determination was done thrice.

Western Blotting and Immunoprecipitation Studies

For Western blot analysis, an equal amount of cell lysate (30–60 $\mu\text{g/well}$, equivalent of 2×10^5 – 4×10^5 cells) was

separated by 10% to 12% SDS-PAGE, which was followed by immunoblotting onto Hybond-P membranes (Amersham Pharmacia Biotech). After blotting in TBST (50 mmol/L Tris-HCl, 150 mmol/L NaCl containing 0.1% Tween 20) with 5% nonfat milk for 1 hour, the membranes were incubated with primary antibodies overnight at 4°C and then with horseradish peroxidase-conjugated secondary antibody for 1 hour at room temperature. Proteins were visualized using the enhanced chemiluminescence detection system (Amersham Pharmacia Biotech).

For the immunoprecipitation studies, 1 mg total protein from cell lysates was incubated overnight with HER2/ ErbB2 primary antibody at 4°C. Protein A/G Plus-agarose (Santa Cruz Biotechnology; 20 μ L of 50% bead slurry) was then added, and the mixture was gently rocked for 2 hours at 4°C. The precipitates were next washed four times with ice-cold lysis buffer, resuspended in 3 \times Laemmli sample buffer, resolved by SDS-PAGE, and immunoblotted with HER2, phospho-HER2, or phosphotyrosine antibodies.

In vitro Kinase Assays

The HER2 *in vitro* kinase reaction was done as described previously (26), with minor modifications. Briefly, MCF7/HER2 cells were lysed in lysis buffer [20 mmol/L Tris (pH 7.5), 150 mmol/L NaCl, 1 mmol/L EDTA, 1 mmol/L EGTA, 1% Triton X-100, 2.5 mmol/L sodium pyrophosphate, 1 mmol/L β -glycerophosphate, 1 mmol/L Na_3VO_4 , 1 μ g/mL leupeptin, 1 mmol/L phenylmethylsulfonyl fluoride]. Total protein lysate (1.5 mg) was precipitated, as described above, with the HER2 antibody (4 μ L) for a 1-hour rotation at 4°C, after which 30 μ L protein A/G Plus-agarose beads was added for an overnight incubation at 4°C. Immunoprecipitates were washed thrice with buffer [50 mmol/L Tris-HCl, 0.5 mol/L LiCl (pH 7.5)] and once with kinase assay buffer [50 mmol/L Tris-HCl (pH 7.5), 10 mmol/L MnCl_2]. Kinase activity was tested by adding 10 μ Ci [γ - ^{32}P]ATP (specific activity, 3,000 Ci/mmol; Amersham Pharmacia Biotech), 10 μ L enolase (stock solution at 2.5 mg/mL), and 10 μ mol/L cold ATP (Sigma Chemical Co., St. Louis, MO) in the presence or absence of the indicated concentrations of CDDO. After 20-minute incubation at room temperature, the reaction was stopped by adding 6 \times Laemmli buffer and heating at 95°C for 5 minutes. Kinase products were resolved by 10% SDS-PAGE, transferred to a nitrocellulose membrane, and exposed to X-ray film. The same nitrocellulose membrane was then rinsed and subjected to a HER2 immunoblotting procedure as described above.

Transient Transfection and Luciferase Activity Assay

One day before transfection, MCF7 cells were seeded in 12-well plates at a density of 0.5×10^5 /mL with DMEM/F12 with 5% fetal bovine serum. Subconfluent cells were transfected with PPREx3-TK-LUC reporter (1 μ g; kindly provided by Dr. Ronald M. Evans, The Salk Institute, La Jolla, CA; ref. 27) and SV- β -galactosidase DNA (0.2 μ g; Promega) using the Fugene-6 transfection reagent (Roche Molecular Biochemicals, Indianapolis, IN) following the manufacturer's instructions. After 24 hours, transfected cells were treated with 2 μ mol/L CDDO or 10 μ mol/L ciglitazone (Cayman Chemical,

Ann Arbor, MI) or with vehicle for 24 hours. Cells were lysed with 200 μ L of 1 \times reporter lysis buffer and cell extracts were subjected to luciferase and β -galactosidase assay. Luciferase activities were normalized to β -galactosidase activity. Each experiment was repeated three to five times.

Quantitative Real-time Reverse Transcription-PCR

Total RNAs were prepared using TRIzol reagent as described by the manufacturer (Life Technologies, Gaithersburg, MD). Total RNA (1 μ g) was reverse transcribed by avian myeloblastosis virus reverse transcriptase (Roche Diagnostic Corp., Chicago, IL) under standard conditions. Duplicate samples of 1 μ L of each cDNA were amplified by PCR in the ABI Prism 7700 Sequence Detection System (PE Applied Biosystems, Foster City, CA). The amplification reaction mixture (25 μ L) contained cDNAs, cyclin D1 primers and probe, and Taqman Universal PCR Master Mix (PE Applied Biosystems). β_2 -Microglobulin was coamplified as an internal control to normalize for variable amounts of cDNA in each sample. The thermocycler variables were as follows: 50°C for 2 minutes, 95°C for 10 minutes, 40 cycles of 95°C for 15 seconds, and 60°C for 1 minute. Results were collected and analyzed to determine the PCR cycle number that generated the first fluorescence signal above a threshold [threshold cycle (C_T); 10 SDs above the mean fluorescence generated during the baseline cycles], after which a comparative C_T method was used to measure relative gene expression. The following formula was used to calculate the relative amount of the transcript of interest in the treated sample (X) and the control sample (Y), both of which were normalized to an endogenous reference value (β_2 -microglobulin): $2^{-\Delta\Delta C_T}$, where ΔC_T is the difference in C_T between the gene of interest and β_2 -microglobulin, with the $\Delta\Delta C_T$ for sample X = $\Delta C_T(X) - \Delta C_T(Y)$.

Northern Blot Analysis

Cells that had been subjected to indicated concentrations of CDDO were lysed in TRIzol, and the total cellular RNA was isolated. The HER2 probe was obtained by cloning the PCR products of amplified cDNA using a pair of HER2 primers. The glyceraldehyde-3-phosphate dehydrogenase probe was used as a loading control. The probes were radiolabeled with [^{32}P]dCTP using the Megaprime DNA Labeling System (Amersham Pharmacia Biotech). Total RNA (10 μ g) was denatured and run for 8 hours on a 1% formamide agarose gel at 30V. After staining in ethidium bromide, RNA was transferred to Hybond-N⁺ membranes (Amersham Pharmacia Biotech). Hybridization was carried out overnight at 68°C in ExpressHyb hybridization solution (Clontech Lab, Chicago, IL). The membranes were washed under highly stringent conditions (0.01 \times SSC and 0.1% SDS for 30 minutes at 65°C) and exposed at -80°C with a double screen to X-ray films (Kodak, Rochester, NY).

Xenograft Studies in Nude Mice

Five-week-old female nude mice (Harlan Sprague-Dawley, Madison, WI) were housed in the barrier and fed with autoclaved diet without phytoestrogens. Animals first implanted with 0.72 mg, 60-day release, 17 β -estradiol pellets (Innovative Research, Sarasota, FL). The next day, 5×10^6 MCF7/Neo or MCF7/HER2 cells suspended

in 300 μ L growth factor–reduced Matrigel (BD Biosciences, Bedford, MA) were injected s.c. in the right flank of each animal. Treatment with CDDO or the liposomal formulation alone (i.e., “empty liposomes”) was initiated once the tumors reached a volume of ≥ 300 mm³.

CDDO was formulated in liposomes at a concentration of 2 mg/mL as follows. First, CDDO was solubilized in *t*-butanol at 37°C at a concentration of 2 mg/mL. Phospholipid distearoyl phosphatidylcholine was solubilized in *t*-butanol at 55°C at a concentration of 10 mg/mL. Distearoyl phosphatidylcholine and CDDO were then mixed together and frozen by being placed at an angle in an acetone and dry ice bath and then quickly turned until the samples were frozen. Samples were then placed on a lyophilizer and freeze-dried overnight. The lipid-to-drug ratio we used was 10:1, 20:1, or 40:1. Empty liposomal controls were made using the same lipids but without CDDO. Liposomal CDDO was reconstituted in normal saline at 55°C to form liposomes and then centrifuged at 13,000 rpm for 1 hour. Pellets were resuspended at room temperature in normal saline at a concentration of 2 mg/mL (100 μ mol/L) for the *in vivo* studies. Liposomal CDDO preparations were centrifuged at 13,000 rpm for 1 hour, and pellets were obtained to determine encapsulation efficiency by liquid chromatography–tandem mass spectrometry. Samples were run on the MicroMass Quattro Ultima (tandem mass spectrometer), and CDDO content in the liposomal CDDO pellets was calculated using the neat standard curve with a quantitation range of 5 to 1,000 ng/mL. Analysis of liposomal preparation pellets (four independent experiments) showed that CDDO was incorporated into distearoyl phosphatidylcholine liposomes at or near the target concentration (range, 83–136 μ mol/L).

Liposomal CDDO was given i.v. thrice weekly via tail vein injection at a final dose 20 mg/kg/mouse/d (0.4 mg/mouse/d in 200 μ L) for 3 weeks. Tumor diameters were serially measured with calipers, and tumor volumes were calculated by the formula: (width² \times length) / 2.

Histology and Immunohistochemistry Analyses

For the histologic analysis, excised tumors were fixed in 10% neutral buffered formalin, embedded in paraffin, sectioned, and stained with H&E. Additional sections were used for immunostaining with cyclin D1 and phospho-HER2 antibodies. Briefly, antigen retrieval was achieved by heating the sections in 10 mmol/L citrate buffer (pH 6.5) in a microwave oven for 20 minutes. Before the sections were stained, endogenous peroxidase was quenched using 3% H₂O₂, and nonspecific binding was blocked using 10% normal goat serum incubated for 1 hour at room temperature. The slides were then incubated with the indicated antibodies overnight at 4°C. The immunostaining was visualized by the avidin-biotin-peroxidase complex method using a Vectastain Elite ABC kit and 3-amino,9-ethyl-carbazole (Vector Laboratories, Burlingame, CA) as chromogen. Slides were counterstained with Mayer’s hematoxylin (Fisher Scientific International, Inc., Pittsburgh, PA). The slides were analyzed under a Nikon Optiphot microscope with a digital capture camera

(Microscopy Documentation System 290, Eastman Kodak, New Haven, CT), and the mean number \pm SD of positive cells was counted from three to five random areas of $\times 20$ field for each slide.

TUNEL Assay

For the *in situ* detection of apoptotic cells in xenograft tumor tissues, a TUNEL assay was done using TUNEL kit (Roche Diagnostics, Mannheim, Germany). Briefly, sections were dewaxed, rehydrated, and digested with 20 μ g/mL proteinase K in 10 mmol/L Tris-HCl buffer for 20 minutes and then treated with permeabilization solution (0.1% Triton X-100 in 0.1% sodium citrate) for 2 minutes on ice. TUNEL reaction mixture (50 μ L) was added to each sample for 30-minute incubation at 37°C. Slides were rinsed with PBS and analyzed by fluorescence microscopy. The mean numbers of apoptotic cells were determined by randomly counting five $\times 20$ fields for each sample.

Statistical Analysis

The results are expressed as mean \pm SD. Levels of significance were evaluated by a two-tailed, paired Student’s *t* test or *F* test (ANOVA), and *P* < 0.05 was considered significant. We did a two-way ANOVA to test for differences among treatments and among cell lines. The model included a term for the interaction between treatment and cell line. We used Tukey’s multiple comparisons procedure to determine how the treatments and cell lines are different if the test from the ANOVA for these effects were significant. This procedure controls the experiment-wise type I error rate (false-positive rate) at 0.05.

For assessment of the *in vivo* xenograft studies, we found the percent change in mean tumor size from baseline (day 1) to each subsequent day when tumor size was measured. A comparative analysis of the percent change in the mean tumor size was fit with a regression model that included terms for treatment, day, and treatment \times day interaction while forcing the intercept term to be 0. A *t* test was used to assess whether each term in the model was statistically significant at the 0.05 level. Data are summarized as mean \pm SD by treatment group or study day as appropriate.

Results

HER2-Overexpressing Breast Cancer Cells Are More Sensitive to Growth-Inhibitory Effects of CDDO

Overexpression of HER2 in transfected MCF7 and MDA-MB-435 cells was confirmed by Western blot analysis (Fig. 1A). Transfection did not significantly change ER status, with MCF7 lines remaining ER positive and MDA-MB-435 cells being ER negative. HER2-transfected MCF7 cells and their vector (control) counterparts were treated with 1 to 5 μ mol/L CDDO. HER2-overexpressing cells were more sensitive to growth-inhibitory effects of CDDO as determined by 3-(4,5-dimethylthiazol-2-yl)-5-(3-carboxymethoxyphenyl)-2-(4-sulfophenyl)-2H-tetrazolium, inner salt assay and IC₅₀ analyses (Fig. 1B); these differences were statistically significant as determined by ANOVA

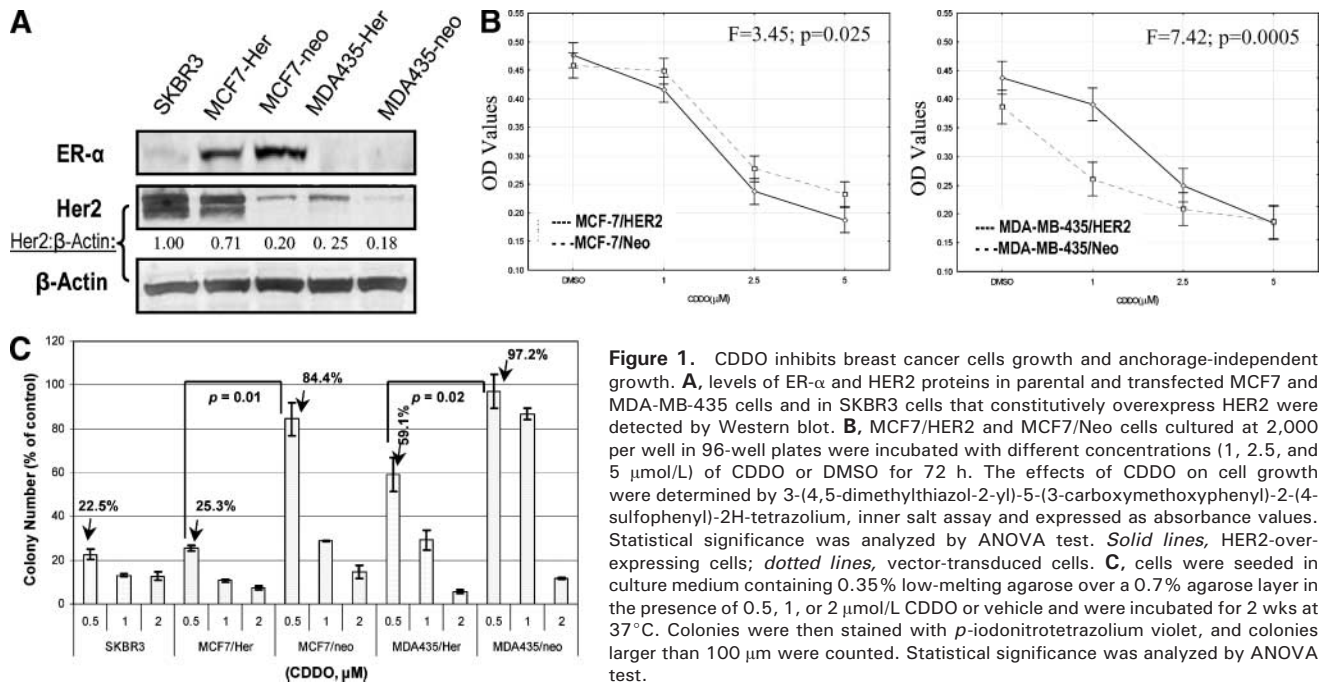


Figure 1. CDDO inhibits breast cancer cells growth and anchorage-independent growth. **A**, levels of ER- α and HER2 proteins in parental and transfected MCF7 and MDA-MB-435 cells and in SKBR3 cells that constitutively overexpress HER2 were detected by Western blot. **B**, MCF7/HER2 and MCF7/Neo cells cultured at 2,000 per well in 96-well plates were incubated with different concentrations (1, 2.5, and 5 $\mu\text{mol/L}$) of CDDO or DMSO for 72 h. The effects of CDDO on cell growth were determined by 3-(4,5-dimethylthiazol-2-yl)-5-(3-carboxymethoxyphenyl)-2-(4-sulfophenyl)-2H-tetrazolium, inner salt assay and expressed as absorbance values. Statistical significance was analyzed by ANOVA test. *Solid lines*, HER2-over-expressing cells; *dotted lines*, vector-transduced cells. **C**, cells were seeded in culture medium containing 0.35% low-melting agarose over a 0.7% agarose layer in the presence of 0.5, 1, or 2 $\mu\text{mol/L}$ CDDO or vehicle and were incubated for 2 wks at 37°C. Colonies were then stained with *p*-iodonitrotetrazolium violet, and colonies larger than 100 μm were counted. Statistical significance was analyzed by ANOVA test.

($P = 0.025$ and $P = 0.0005$, respectively, in MCF7 and MDA-MB-435 cells). The IC_{50} s were 3.53 ± 0.17 and 4.03 ± 0.12 $\mu\text{mol/L}$, respectively, in MCF7/HER2 and MCF7/Neo cells ($P = 0.002$); 3.86 ± 0.15 and 7.47 ± 1.04 $\mu\text{mol/L}$, respectively, in MDA-MB-435/HER2 and MDA-MB-435/Neo cells ($P = 0.018$).

To determine whether CDDO affects anchorage-independent cell growth, an important hallmark of cell transformation, we monitored colony formation in soft agarose. A two-way ANOVA was used to compare the differences among different concentrations of CDDO (0.5, 1.0, and 2.0 $\mu\text{mol/L}$) and among cell lines (MCF7/HER, MCF7/Neo, MDA-MB-435/HER, and MDA-MB-435/Neo). This analysis revealed that there are differences among the treatments ($P < 0.001$), and there are differences among the cell lines ($P < 0.001$). When a term for the interaction between cell line and treatment was included in the ANOVA model, this term was also statistically significant ($P < 0.001$), suggesting that the treatments have different effects in different cell lines. Tukey's multiple comparisons test revealed that all three treatments are different from one another ($P = 0.002$), with means of 66.514 (CDDO 0.5 $\mu\text{mol/L}$), 38.787 (CDDO 1.0 $\mu\text{mol/L}$), and 9.870 (CDDO 2.0 $\mu\text{mol/L}$). Tukey's multiple comparisons procedure also revealed that all four cell lines are significantly different from one another ($P < 0.001$), with means of 65.196 (MDA-MB-435/Neo), 31.370 (MDA-MB-435/HER), 42.579 (MCF7/Neo), and 14.416 (MCF7/HER). This analysis shows that the colony-forming activity of HER2-overexpressing breast cancer cells is significantly more suppressed than that of nonoverexpressing cell lines. The size of colony was profoundly diminished in HER2-overexpressing MCF7 and MDA-MB-435 cells compared

with their vectors (control) counterparts (data not shown). At ≥ 2 $\mu\text{mol/L}$ CDDO, colony formation was almost completely suppressed in all the cell lines tested. This finding implies that at low concentrations of CDDO HER2 is likely to be the primary target for the reduction of colony formation. At higher concentrations of CDDO, other mechanisms may apply, such as cell cycle regulation and/or an induction of apoptosis.

CDDO Inhibits HER2 Phosphorylation and Decreases HER2 Kinase Activity and Protein Level

To determine if preferential inhibition of HER2-over-expressing cells by CDDO is associated with potential effects of the compound on HER2 signaling, we examined the effects of CDDO on HER2 phosphorylation and tyrosine kinase activity. CDDO treatment (1 hour) inhibited phosphotyrosine content of HER2 in MCF7/HER2 cells along with specific phosphorylation of the 1248 site of HER2 (Fig. 2A).

An immunocomplex kinase assay was then done to examine the effects of CDDO on the tyrosine kinase activity of HER2. Immunoprecipitates of lysates of MCF7/HER2 cells were incubated in the presence of varying concentrations of CDDO or vehicle. Both the autophosphorylation of HER2 and the transphosphorylation of an exogenous substrate, enolase, were partially inhibited by CDDO (Fig. 2B). Time-course analysis further showed that CDDO decreased the levels of total HER2 protein in MCF7/HER2 cells at 24 and 48 hours in a dose-dependent fashion, but this effect was apparent only at high (> 5 $\mu\text{mol/L}$) concentrations of CDDO (Fig. 2C). No effect on HER2 mRNA was seen at 24 hours as shown by Northern blot analysis (Fig. 2D). These results suggest that CDDO represses the intrinsic tyrosine kinase activity of HER2

and subsequently reduces total HER2 protein levels. To investigate the possibility that CDDO induces the proteasomal degradation of HER2, cells were pretreated with the proteasome inhibitors MG132 or proteasome inhibitor I and then exposed to CDDO. Both proteasome inhibitors prevented a decrease in the level of HER2 protein (Fig. 2E), suggesting that CDDO indeed induces the proteasomal degradation of the receptor. However, proteasome inhibitors failed to restore cyclin D1 levels.

PPAR γ -Dependent Transactivation by CDDO in Breast Cancer Cells

To determine if the putative target of CDDO, PPAR γ , is modulated by CDDO in HER2-overexpressing cells, we transfected MCF7/Neo and MCF7/HER2 cells with a PPRE-Luc construct and measured the luciferase activity.

PPAR γ protein was expressed in both MCF7/Neo and MCF7/HER2 cells although at higher levels in the MCF7/HER2 cells (Fig. 3A). We compared transcriptional activation of the receptor in both cell lines by CDDO and PPAR γ ligand ciglitazone (Fig. 3B). A two-way ANOVA that included a term for the interaction between cell line and treatment was done to test for differences among treatments (CDDO 2.0 μ mol/L, ciglitazone 10.0 μ mol/L, and DMSO) and between cell lines (MCF7/HER and MCF7/Neo). This analysis revealed that there are differences among the treatments ($P < 0.001$), and the treatments have different effects in different cell lines ($P < 0.001$). A one-way ANOVA was then used to compare the transcriptional activation of PPAR γ by CDDO or ciglitazone within each cell line. For both cell lines, there was a statistically

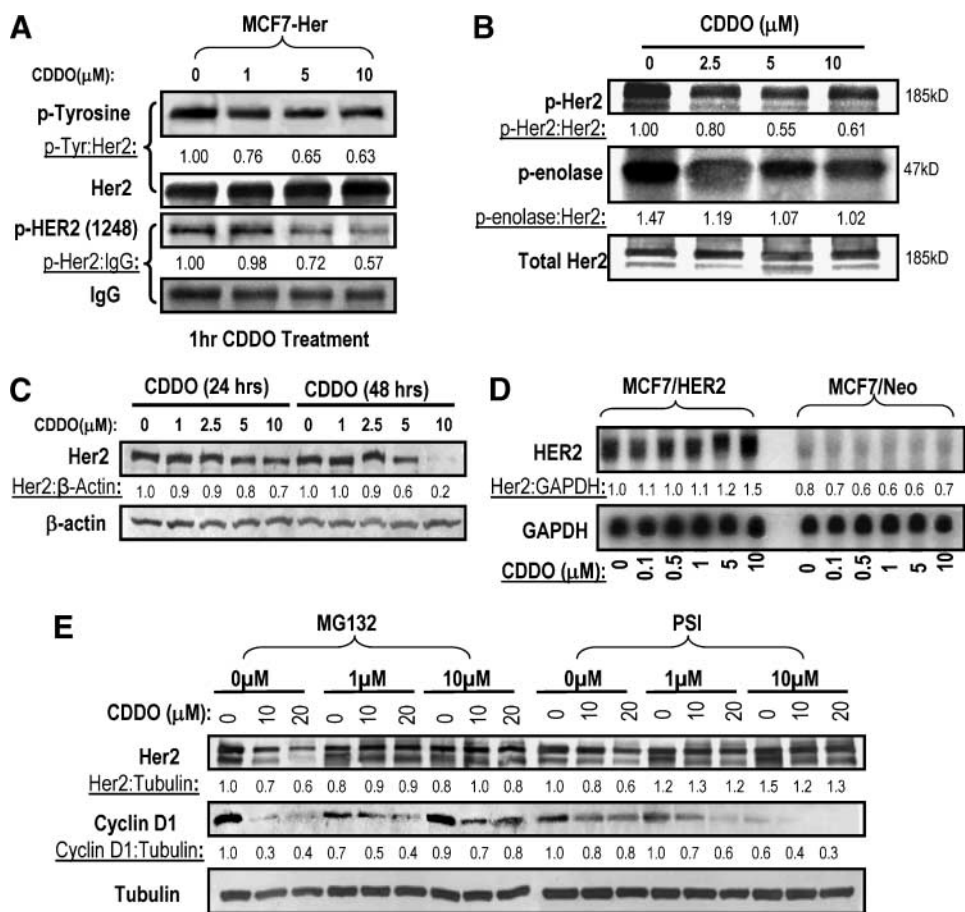


Figure 2. CDDO decreases HER2 activation and protein level. **A**, MCF7/HER2 cells were incubated with DMSO or increasing concentrations of CDDO (1, 5, and 10 μ mol/L) for 1 h. Cell extracts were immunoprecipitated with the anti-HER2 antibody and then immunoblotted with either anti-phosphotyrosine antibody (*p-Tyrosine*), phosphospecific HER2 antibody [*p-HER (1248)*], or anti-HER2 antibody. IgG as a loading control. Densitometric analysis was done as described in Materials and Methods. *Numbers*, ratios of phospho-HER2 to total HER2. **B**, cell lysates from untreated MCF7/HER2 cells were immunoprecipitated with the anti-HER2 antibody. Kinase activity was measured by incubation with [γ - 32 P]ATP, enolase, and varying concentrations of CDDO for 20 min. Reactants were resolved on 10% SDS-PAGE and transferred to nitrocellulose, and the phosphorylation products were visualized by autoradiography. Total HER2 was detected by Western blot as a loading control. **C**, MCF7/HER2 cells were exposed to the indicated concentrations of CDDO or DMSO for 24 or 48 h and then harvested for Western blot analysis with anti-HER2 antibody. **D**, Northern blot in which HER2 and glyceraldehyde-3-phosphate dehydrogenase (*GAPDH*) probes were used for detecting mRNA levels of MCF7/HER2 and MCF7/Neo cells treated with the indicated concentrations of CDDO for 24 h. **E**, CDDO-induced HER2 down-regulation is partially inhibited by proteasome inhibitors. MCF7/HER2 cells were pretreated for 1 h with the indicated concentrations of the proteasome inhibitors MG132 or proteasome inhibitor I followed by exposure to CDDO for 16 h, and cell lysates were analyzed by Western blot.

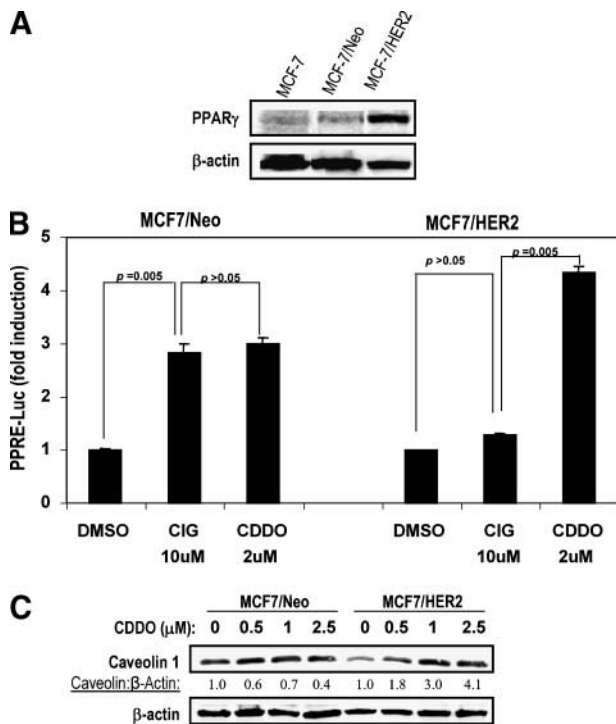


Figure 3. **A**, expression of PPAR γ in parental MCF7 cells, MCF7/Neo vector control cells, and MCF7/HER2 cells as shown by Western blot analysis using a monoclonal antibody to PPAR γ . The monoclonal antibody reacts with both PPAR γ 1 and PPAR γ 2 isoforms. **B**, MCF7/Neo and MCF7/HER2 cells were transiently transfected with 1 μ g TK-PPRE-Luc construct. After 24 h, transfected cells were treated with 2 μ mol/L CDDO or 10 μ mol/L ciglitazone (CIG), and luciferase activity was determined as described in Materials and Methods. Columns, mean ($n = 3$); bars, SD. **C**, MCF7/Neo and MCF7/HER2 cells were treated with indicated concentrations of CDDO for 24 h, and caveolin-1 expression was determined by Western blot analysis.

significant difference among the treatment groups ($P = 0.002$ and $P < 0.001$ for MCF7/Neo and MCF7/HER2, respectively). In MCF7/Neo cells, comparison by Tukey's multiple comparisons procedure revealed that 2.0 μ mol/L CDDO and 10.0 μ mol/L ciglitazone were not significantly different from one another but that both of these treatments were significantly different from DMSO ($P = 0.005$). In MCF7/HER2, 2.0 μ mol/L CDDO was significantly different from both 10.0 μ mol/L ciglitazone and DMSO ($P = 0.005$) but that 10.0 μ mol/L ciglitazone and DMSO were not significantly different from one another. These data suggest that CDDO activates PPAR γ signaling in both HER2-positive and HER2-negative cells. In contrast, the PPAR γ ligand ciglitazone at 10 μ mol/L induced increased luciferase activity in MCF7 (parental) and MCF7/Neo cells but not in MCF7/HER2 cells, consistent with previously published results (28).

Caveolin-1 is a potent suppressor of mammary tumor growth and metastasis (29), and recent studies have shown that caveolins are induced in cancer cells when PPAR γ is ligated (30–32). Because caveolin-1 negatively regulates the activation of diverse kinases, including HER2 (33), and the

activation of PPAR γ has been reported to inhibit neuregulin-induced HER2 tyrosine phosphorylation (17), we examined the effects of CDDO on caveolin-1 expression in breast cancer cells. MCF7/HER2 cells expressed caveolin-1 at significantly lower levels than MCF7/Neo controls, consistent with published reports (ref. 33; Fig. 3C). CDDO consistently induced caveolin-1 protein expression in both cell lines at 24 hours, restoring caveolin-1 expression in MCF7/HER2 cells to the levels in vector-transduced cells (Fig. 3C).

We showed previously that CDDO down-regulates cyclin D1 in breast cancer cells (24). In this study, we have now extended our analysis to cells overexpressing HER2. By using quantitative real-time PCR, we were able to determine that CDDO down-regulated cyclin D1 mRNA at 24 hours in a dose-dependent fashion in both MCF7/Neo and MCF7/HER2 cells (Fig. 4A), with the complete disappearance of cyclin D1 protein at 5 and 10 μ mol/L CDDO (Fig. 4B). However, this effect was not seen at lower (1 and 2.5 μ mol/L) concentrations of CDDO (data not shown). No change in cyclin E expression was noted.

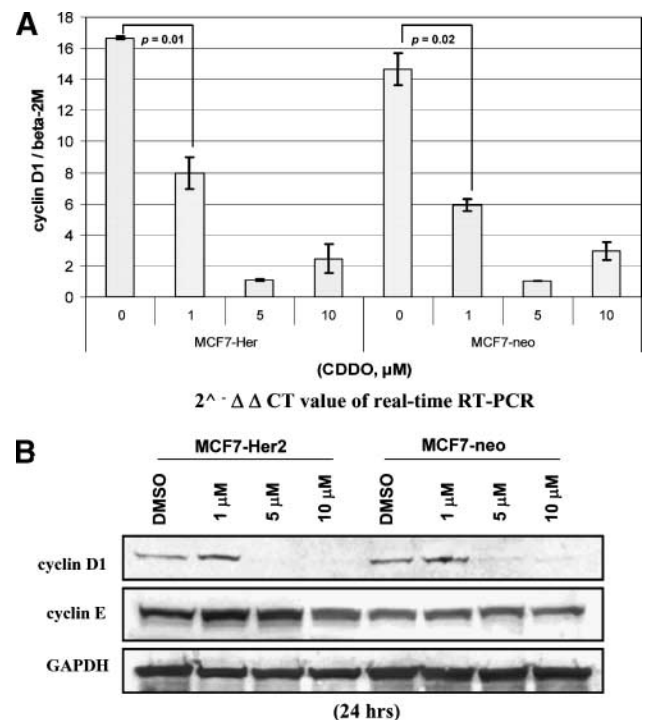


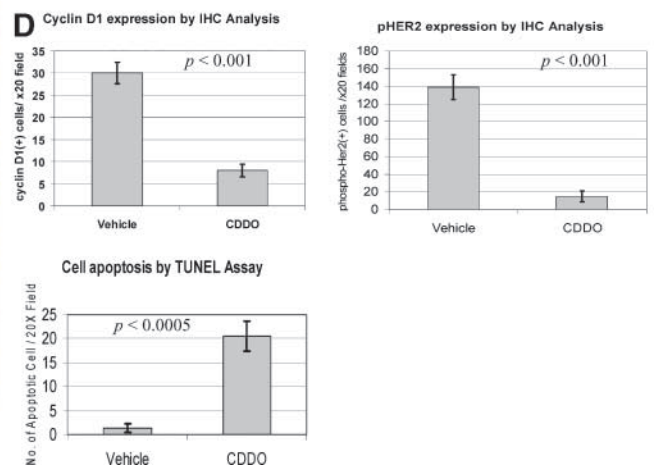
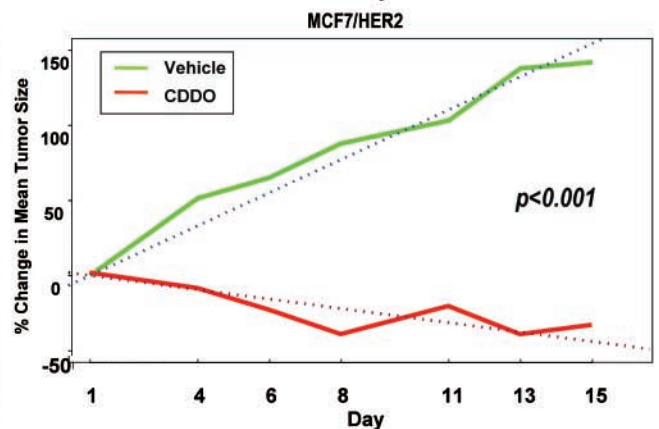
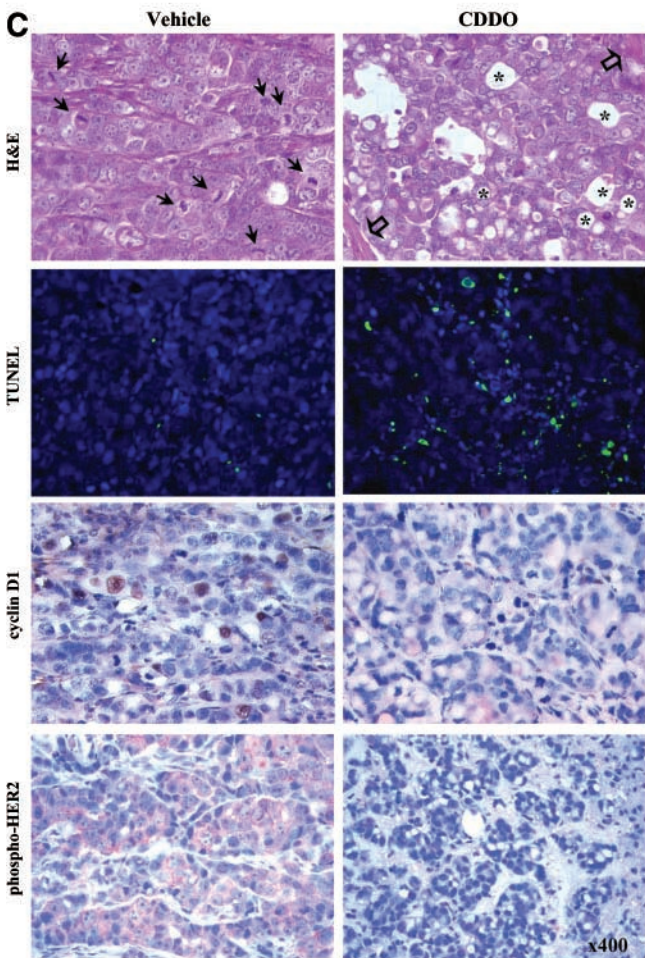
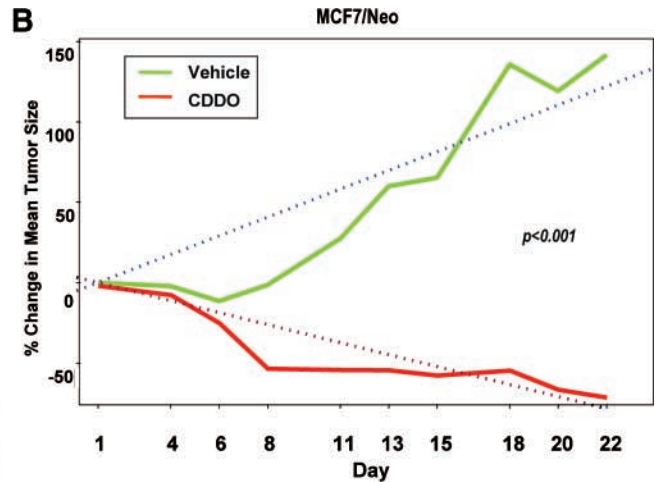
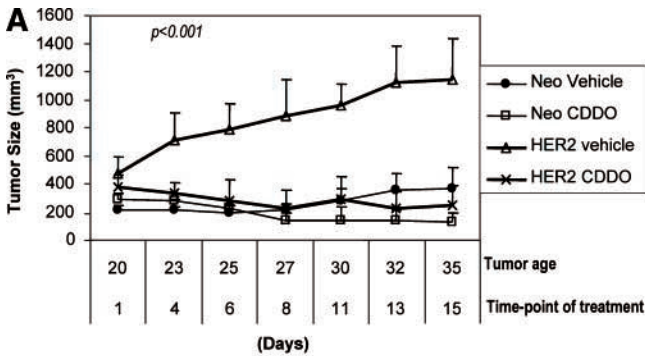
Figure 4. CDDO induces cyclin D1 down-regulation in MCF7/Neo and MCF7/HER2 cells. **A**, breast cancer cells were exposed to the indicated concentrations of CDDO or vehicle for 24 h. RNA extraction and real-time PCR were done to determine the effects of each concentration of CDDO. Each sample was normalized to β_2 -microglobulin, and results were expressed as a fold change. **B**, in the same experiment, cells were harvested and lysed for Western blot analysis. Western blot analysis confirmed the results of real-time PCR at the protein level, with the down-regulation of cyclin D1 and no change in cyclin E expression.

CDDO Reduces HER2-Positive Breast Cancer Growth in Immunodeficient Mice

We then tested the antitumor effects of CDDO *in vivo* in a murine breast cancer xenograft model. At the start of therapy, MCF7/HER2 tumors were twice as large as MCF7/Neo tumors and continued to grow faster. However, CDDO abrogated the growth of both tumor types compared with the tumors in control mice treated with vehicle alone

(Fig. 5A). Indeed, there was a statistically significant difference ($P < 0.001$) in the rate of tumor growth and the percentage of change in the mean tumor sizes over time between the two treatment groups (vehicle and CDDO), with the same conclusion reached in mice with either MCF7/Neo or MCF7/HER2 tumors (Fig. 5B).

We then analyzed the histologic appearance of tumors collected from the mice following treatment. Microscopically,



changes secondary to CDDO treatment include inconspicuous mitotic figures and reduced nucleocytoplasmic ratio, tumor tissue replacement by distinct fibrosis that trend to confluence and separate the tumor mass into multifocal nest structures, formation of ductal lumen-like structure (Fig. 5C, H&E), accumulation of foamy cytoplasm in tumor cells, and inflammatory cell infiltration (data not shown). Furthermore, CDDO significantly ($P < 0.001$) decreased HER2 phosphorylation and nuclear cyclin D1 expression in tumors as determined by immunohistochemistry analysis (Fig. 5C and D). TUNEL assay showed that CDDO treatment induced tumor cell apoptosis (Fig. 5C, TUNEL), which was 7-fold higher in CDDO-treated compared with vehicle-treated group (Fig. 5C and D; $P < 0.0005$).

Discussion

In this study in which we examined the antitumor effect of the triterpenoid CDDO on human breast cancer cells engineered to overexpress the HER2/*neu* gene, CDDO inhibited the growth of cells overexpressing HER2 at concentrations lower than those required to inhibit the growth of vector control cells. We further found *in vitro* that CDDO inhibited HER2 autophosphorylation and transphosphorylation. The concentrations of CDDO required for the inhibition of kinase activity were in the same range as concentrations that inhibit breast cancer cell growth. At 0.5 and 1 $\mu\text{mol/L}$, the colony formation of HER2-overexpressing cell lines was significantly more suppressed than that of the nonoverexpressing cell lines in soft agar. At higher concentrations, the colony-forming ability was almost completely suppressed, regardless of the level of HER2 expression. At high concentrations, CDDO decreased the total HER2 levels likely by proteasome-dependent degradation. It has been reported that the degradation of HER2 by 17-allylamino,17-demethoxygeldanamycin in parental MCF7 cells expressing low HER2 levels was not sufficient to arrest cell growth but caused the death of cells that depended on HER2 signaling (34). These collective data suggest that although CDDO preferentially suppresses the growth and transformation ability of HER2-overexpressing cancer cells at lower concentrations, other effects of CDDO may account for its inhibitory effect on growth of cell lines expressing the basal level of HER2.

CDDO reportedly binds to and transactivates PPAR γ (14), and we have reported that CDDO activates PPAR γ in leukemic cells (23) and breast cancer cells (24). In keeping with this, human breast cancer cells express high levels of PPAR γ and are functionally responsive to synthetic and natural ligands (35, 36). Moreover, PPAR γ is expressed in both primary and metastatic breast cancer, where its transactivation has been reported to induce growth arrest and apoptosis (37) and to mediate the transcription of target genes that are associated with a more differentiated, less malignant phenotype (38). Recent studies have further shown that the overexpression of PPAR γ in breast cancer cells is caused by a tumor-specific promoter that is distinct from the promoter used in normal epithelial cells (39). PPAR γ has also been suggested to be a crucial gene for regulating BRCA1 gene expression, which might therefore make it important in the BRCA1 regulatory pathway that is involved in the pathogenesis of sporadic breast cancer (40).

A recent study showed that PPAR γ levels are up-regulated in cells that overexpress HER2, but this was associated with resistance to the growth-inhibitory effects of the bona fide PPAR γ ligand troglitazone unless it was combined with trastuzumab (Herceptin; ref. 28). Consistent with these findings, we also observed higher PPAR γ protein levels in MCF7/HER2 cells than in MCF7/Neo cells. Furthermore, ciglitazone, another PPAR γ ligand from the thiazolidinedione class, failed to activate PPAR γ . In contrast, CDDO induced PPAR γ -dependent transactivation in both HER2-transfected and vector control cells. This difference in tissue/cell selectivity between CDDO and thiazolidinediones in their PPAR γ -dependent responses may result from the unique ability of CDDO to recruit different classes of coactivators. As such, our data in colon cancer cells showed recruitment of multiple coactivators (Src-1, Src-2, Src-3, TRAP220/DRIP205, CARM-1, and PGC-1) that is qualitatively different from that induced by other PPAR γ ligands (41).

We recently identified the cell cycle regulator genes cyclin D1 and p21 as transcriptional targets of CDDO in breast cancer (24). Similar to its effects in other cell lines, in the present study, we observed that CDDO down-regulated cyclin D1 expression at both mRNA and protein levels in MCF7/HER2 cells. Cyclin D1 is a major regulator of G₁

Figure 5. Effect of CDDO on breast cancer *in vivo*. **A**, female nude mice were inoculated s.c. with estrogen-releasing pellets and with 5×10^6 MCF7/HER2 or MCF7/Neo cells. Twenty days after inoculation, five MCF7/Neo-injected mice and eight MCF7/HER2-injected mice were treated with liposomally encapsulated CDDO (20 mg/kg/d i.v. thrice weekly for 3 wks). Eleven mice (4 injected with MCF7/Neo and 7 injected with MCF7/HER2 cells) received vehicle only. The tumor was measured twice weekly with microcalipers, and the tumor volume was calculated. **B**, percent change in the mean tumor size over time in the mice injected with MCF7/Neo cells (*top*) and MCF7/HER2 cells (*bottom*). *Green lines*, percent change in the mean tumor size each day in the mice treated with vehicle; *red lines*, percent change in the mean tumor size each day in the mice treated with CDDO; *dotted line*, regression line obtained when the percent change in the mean tumor size is fit with a simple linear model over days, with the intercept term forced to be 0. **C**, tumors from mice that received vehicle control or CDDO were excised and stained with H&E, TUNEL, or antibodies against cyclin D1 and phospho-HER2. Microscopically, tumor cells from vehicle-treated animals appeared larger with high nucleocytoplasmic ratio and increased mitotic figures (*closed arrowheads*). Tumor cells from mice treated with CDDO showed reduced nucleocytoplasmic ratio and mitotic figures. Tumor tissue is replaced by distinct loose fibrosis (*open arrows*) and formed ductal lumen-like structure (*asterisks*), and the number of apoptotic cells is increased (*green signal* in TUNEL staining). Immunohistochemically, positive signal (*brown staining*) of cyclin D1 was mostly of nuclear localization and positive signal (*brown staining*) of phospho-HER2 was located on cell membrane. Tumor cells after CDDO treatment showed weak or lack of positive signals of cyclin D1 and phospho-HER2. **D**, cyclin D1 and phospho-HER2 expression (IHC) and cell apoptosis (TUNEL) were analyzed as described in Materials and Methods. *Columns*, mean number of positive cells was counted in three to five random areas of $\times 20$ field for each sample; *bars*, SD. Results were compared by *t* test.

cell cycle progression, with up to 40% of human breast cancers showing overexpression or amplification of cyclin D1 (42, 43). Cyclin D1 in the mammary gland is required for the development of HER2/*neu*- or Ras-induced breast cancers (44). Conversely, cyclin D1 antisense abolished the growth of Neu-transformed mammary cells in immunodeficient mice (45). Further, Wang et al. (46) reported that 15-deoxy- Δ 12,14-prostaglandin J2 decreased cyclin D1 mRNA and protein levels in MCF7 cells, and their studies indicated that this transcriptional inhibition was due to competition between PPAR γ and c-fos (bound to the cyclin D1 promoter) for limiting cellular levels of p300, an important coregulatory protein. In another study, 15-deoxy- Δ 12,14-prostaglandin J2 and ciglitazone decreased cyclin D1 protein levels by the proteasome-dependent degradation of cyclin D1 (47). In the present study, CDDO caused the down-regulation of cyclin D1 protein at concentrations higher than those required to inhibit cell growth, indicating that this response was PPAR γ independent as was also reported for 15-deoxy- Δ 12,14-prostaglandin J2 and substituted diindolymethane derivatives in MCF7 cells (21, 48, 49). However, unlike other PPAR γ ligands (47), CDDO did not induce the degradation of cyclin D1 via the ubiquitin-proteasome pathway as shown by the fact that the proteasome inhibitors MG132 and proteasome inhibitor I failed to restore cyclin D1 expression. These observations clearly distinguish between the PPAR γ -independent responses induced by CDDO and by other structural classes of PPAR γ agonists.

Caveolin-1 recently emerged as a potential downstream target of the PPAR γ gene in several cellular systems. Caveolin-1, the principal structural component of the caveolae membrane domains in mammary epithelial cells, is a potent suppressor of mammary tumor growth and metastasis (29, 50). Caveolins may function as negative regulators of signal transduction through their direct interactions with caveolae-associated signaling molecules, such as Ha-Ras, epidermal growth factor receptor, protein kinase C, Src family kinases, and others (51–53), and recent studies have shown a reciprocal relationship between the HER2 tyrosine kinase activity and caveolin-1 protein expression (33). Further, caveolin-1 transcriptionally controls cyclin D1 levels in different cell types (54). Because several studies (30–32) have shown that caveolins are modulated via PPAR γ ligation, we examined the effects of CDDO on caveolin-1 expression in breast cancer cells. CDDO significantly induced caveolin-1 expression in both MCF7/Neo and MCF7/HER2 cells in only 24 hours and thereby restored caveolin-1 expression in HER2 transfectants with low baseline levels. Because caveolin-1 exhibits tumor-suppressing and growth-inhibitory activities, these results suggest that the induction of caveolin-1 is important for the antiproliferative effects of PPAR γ -active CDDO in breast cancer. We have recently reported that CDDO-induced growth inhibition of colon cancer cell correlated with induction of caveolin-1 in PPAR γ -dependent

fashion (41). Further studies will need to be done to determine whether the induction of caveolin-1 by CDDO is responsible for the inhibition of HER2 tyrosine activity and cyclin D1 down-regulation. Of relevance, the natural PPAR γ ligand 15-deoxy- Δ 12,14-prostaglandin J2 was shown to block the phosphorylation of HER2 and other receptor tyrosine kinases, such as insulin-like growth factor-1 receptor (17). However, our results show that CDDO directly inhibits HER2-dependent phosphorylation activity *in vitro* (Fig. 5B), suggesting that this inhibitory response is also PPAR γ independent.

Several studies have shown the chemopreventive activity of PPAR γ ligands in chemically induced mammary tumors, an activity that was enhanced by retinoid X receptor ligation (55–57). Our study provides the first *in vivo* evidence of the antitumor activity of liposomally delivered CDDO in a xenograft model of breast cancer. CDDO completely abrogated the growth of both MCF7/Neo and MCF7/HER2 tumors in an immunodeficient mouse model. This is particularly notable because the MCF7/HER2 cells otherwise grew very rapidly, requiring the sacrifice of animals in the control group by day 35. Importantly, we also showed that CDDO down-regulates cyclin D1 and phospho-HER2 expression and induces tumor cell apoptosis *in vivo*, which was consistent with our *in vitro* data. Morphologically, tumors exhibited reduced nucleocytoplasmic ratio and lower mitotic index, consistent with the low cyclin D1 expression level. Tumor cells also contained clear vacuolated or foamy cytoplasm after CDDO treatment. These results suggest that CDDO may be beneficial for treatment of patients with breast cancer involving HER2 amplification, which is historically an aggressive disease associated with short survival. Further recommending CDDO for clinical use, CDDO showed a favorable toxicity and pharmacokinetic profile in preclinical studies conducted at the National Cancer Institute (58), and clinical phase I trials of CDDO in patients with hematopoietic malignancies and solid tumors have been planned.

Acknowledgments

We thank Rosemarie Lauzon for help in the preparation of the article.

References

- Slamon DJ, Clark GM, Wong SG, et al. Human breast cancer: correlation of relapse and survival with amplification of the HER-2/*neu* oncogene. *Science* 1987;235:177–82.
- Kurokawa H, Lenferink AEG, Simpson JF, et al. Inhibition of HER2/*neu* (erbB-2) and mitogen-activated protein kinases enhances tamoxifen action against HER2-overexpressing, tamoxifen-resistant breast cancer cells. *Cancer Res* 2000;60:5887–94.
- Yu D, Jing T, Liu B, et al. Overexpression of ErbB2 blocks Taxol-induced apoptosis by upregulation of p21Cip1, which inhibits p34Cdc2 kinase. *Mol Cell* 1998;2:581–91.
- Slamon DJ, Leyland-Jones B, Shak S, et al. Use of chemotherapy plus a monoclonal antibody against HER2 for metastatic breast cancer that overexpresses HER2. *N Engl J Med* 2001;344:783–92.
- Suh WS, Kim YS, Schimmer AD, et al. Synthetic triterpenoids activate a pathway for apoptosis in AML cells involving downregulation of FLIP and sensitization to TRAIL. *Leukemia* 2003;17:2122–9.

6. Ito Y, Pandey P, Place A, et al. The novel triterpenoid 2-cyano-3,12-dioxoolean-1,9-dien-28-oic acid induces apoptosis of human myeloid leukemia cells by a caspase-8-dependent mechanism. *Cell Growth Differ* 2000;11:261–7.
7. Inoue S, Snowden RT, Dyer MJ, Cohen GM. CDDO induces apoptosis via the intrinsic pathway in lymphoid cells. *Leukemia* 2004;18:948–52.
8. Chauhan D, Li G, Podar K, et al. The bortezomib/proteasome inhibitor PS-341 and triterpenoid CDDO-lm induce synergistic anti-multiple myeloma (MM) activity and overcome bortezomib resistance. *Blood* 2004;103:3158–66.
9. Ikeda T, Nakata Y, Kimura F, et al. Induction of redox imbalance and apoptosis in multiple myeloma cells by the novel triterpenoid 2-cyano-3,12-dioxoolean-1,9-dien-28-oic acid. *Mol Cancer Ther* 2004;3:39–45.
10. Kim KB, Lotan R, Yue P, et al. Identification of a novel synthetic triterpenoid, methyl-2-cyano-3,12-dioxooleana-1,9-dien-28-oate, that potently induces caspase-mediated apoptosis in human lung cancer cells. *Mol Cancer Ther* 2002;1:177–84.
11. Melichar B, Konopleva M, Hu W, et al. Growth-inhibitory effect of a novel synthetic triterpenoid, 2-cyano-3,12-dioxoolean-1,9-dien-28-oic acid, on ovarian carcinoma cell lines not dependent on peroxisome proliferator-activated receptor- γ expression. *Gynecol Oncol* 2004;93:149–54.
12. Ito Y, Pandey P, Sporn MB, et al. The novel triterpenoid CDDO induces apoptosis and differentiation of human osteosarcoma cells by a caspase-8 dependent mechanism. *Mol Pharmacol* 2001;59:1094–9.
13. Place AE, Suh N, Williams CR, et al. The novel synthetic triterpenoid, CDDO-imidazolide, inhibits inflammatory response and tumor growth *in vivo*. *Clin Cancer Res* 2003;9:2798–806.
14. Wang Y, Porter WW, Suh N, et al. A synthetic triterpenoid, 2-cyano-3,12-dioxooleana-1,9-dien-28-oic acid (CDDO), is a ligand for the peroxisome proliferator-activated receptor γ . *Mol Endocrinol* 2000;14:1550–6.
15. Mueller E, Sarraf P, Tontonoz P, et al. Terminal differentiation of human breast cancer through PPAR γ . *Mol Cell* 1998;1:465–70.
16. Tontonoz P, Singer S, Forman BM, et al. Terminal differentiation of human liposarcoma cells induced by ligands for peroxisome proliferator-activated receptor γ and the retinoid X receptor. *Proc Natl Acad Sci U S A* 1997;94:237–41.
17. Pignatelli M, Cortes-Canteli M, Lai C, Santos A, Perez-Castillo A. The peroxisome proliferator-activated receptor γ is an inhibitor of ErbBs activity in human breast cancer cells. *J Cell Sci* 2001;114:4117–26.
18. Palakurthi SS, Aktas H, Grubisich LM, Mortensen RM, Halperin JA. Anticancer effects of thiazolidinediones are independent of peroxisome proliferator-activated receptor γ and mediated by inhibition of translation initiation. *Cancer Res* 2001;61:6213–8.
19. Baek SJ, Wilson LC, Hsi LC, Eling TE. Troglitazone, a peroxisome proliferator-activated receptor γ (PPAR γ) ligand, selectively induces the early growth response-1 gene independently of PPAR γ . A novel mechanism for its anti-tumorigenic activity. *J Biol Chem* 2003;278:5845–53.
20. Kim JA, Park KS, Kim HI, et al. Troglitazone activates p21Cip/WAF1 through the ERK pathway in HCT15 human colorectal cancer cells. *Cancer Lett* 2002;179:185–95.
21. Qin C, Morrow D, Stewart J, et al. A new class of peroxisome proliferator-activated receptor γ (PPAR γ) agonists that inhibit growth of breast cancer cells: 1,1-bis(3'-indolyl)-1-(*p*-substituted phenyl)methanes. *Mol Cancer Ther* 2004;3:247–60.
22. Konopleva M, Tsao T, Estrov Z, et al. The synthetic triterpenoid 2-cyano-3,12-dioxooleana-1,9-dien-28-oic acid induces caspase-dependent and -independent apoptosis in acute myelogenous leukemia. *Cancer Res* 2004;64:7927–35.
23. Konopleva M, Elstner E, McQueen TJ, et al. Peroxisome proliferator-activated receptor γ and retinoid X receptor ligands are potent inducers of differentiation and apoptosis in leukemias. *Mol Cancer Ther* 2004;3:1249–62.
24. Lapillonne H, Konopleva M, Tsao T, et al. Activation of peroxisome proliferator-activated receptor γ by a novel synthetic triterpenoid 2-cyano-3,12-dioxooleana-1,9-dien-28-oic acid induces growth arrest and apoptosis in breast cancer cells. *Cancer Res* 2003;63:5926–39.
25. Yu D, Liu B, Tan M, et al. Overexpression of c-erbB-2/*neu* in breast cancer cells confers increased resistance to Taxol via mdr-1-independent mechanisms. *Oncogene* 1996;13:1359–65.
26. Hong RL, Spohn WH, Hung M-C. Curcumin inhibits tyrosine kinase activity of p185neu and also depletes p185neu. *Clin Cancer Res* 1999;5:1884–91.
27. Forman BM, Tontonoz P, Chen J, et al. 15-Deoxy-12,14 prostaglandin J2 is a ligand for the adipocyte determination factor PPAR. *Cell* 1995;83:803–12.
28. Yang Z, Bagheri-Yarmand R, Balasenthil S, et al. HER2 regulation of peroxisome proliferator-activated receptor γ (PPAR γ) expression and sensitivity of breast cancer cells to PPAR γ ligand therapy. *Clin Cancer Res* 2003;9:3198–203.
29. Williams TM, Medina F, Badano I, et al. Caveolin-1 gene disruption promotes mammary tumorigenesis and dramatically enhances lung metastasis *in vivo*. Role of Cav-1 in cell invasiveness and matrix metalloproteinase (MMP-2/9) secretion. *J Biol Chem* 2004;279:51630–46.
30. Burgermeister E, Tencer L, Liscovitch M. Peroxisome proliferator-activated receptor- γ upregulates caveolin-1 and caveolin-2 expression in human carcinoma cells. *Oncogene* 2003;22:3888–900.
31. Chintharlapalli S, Smith R III, Samudio I, Zhang W, Safe S. 1,1-Bis(3'-indolyl)-1-(*p*-substituted phenyl)methanes induce peroxisome proliferator-activated receptor γ -mediated growth inhibition, transactivation, and differentiation markers in colon cancer cells. *Cancer Res* 2004;64:5994–6001.
32. Bender FC, Reymond MA, Bron C, Quest AF. Caveolin-1 levels are down-regulated in human colon tumors, and ectopic expression of caveolin-1 in colon carcinoma cell lines reduces cell tumorigenicity. *Cancer Res* 2000;60:5870–8.
33. Engelman JA, Lee RJ, Karnezis A, et al. Reciprocal regulation of neu tyrosine kinase activity and caveolin-1 protein expression *in vitro* and *in vivo*. Implications for human breast cancer. *J Biol Chem* 1998;273:20448–55.
34. Munster PN, Marchion DC, Basso AD, Rosen N. Degradation of HER2 by ansamycins induces growth arrest and apoptosis in cells with HER2 overexpression via a HER3, phosphatidylinositol 3'-kinase-AKT-dependent pathway. *Cancer Res* 2002;62:3132–7.
35. Kilgore MW, Tate PL, Pai S, Sengoku E, Price TM. MCF-7 and T47D human breast cancer cells contain a functional peroxisomal response. *Mol Cell Endocrinol* 1997;129:229–35.
36. Thoennes SR, Tate PL, Price TM, Kilgore MW. Differential transcriptional activation of peroxisome proliferator-activated receptor γ by ω -3 and ω -6 fatty acids in MCF-7 cells. *Mol Cell Endocrinol* 2000;160:67–73.
37. Elstner E, Muller C, Koshizuka K, et al. Ligands for peroxisome proliferator-activated receptor γ and retinoic acid receptor inhibit growth and induce apoptosis of human breast cancer cells *in vitro* and in BNX mice. *Proc Natl Acad Sci U S A* 1998;95:8806–11.
38. Mueller E, Sarraf P, Tontonoz P, et al. Terminal differentiation of human breast cancer through PPAR γ . *Mol Cell* 1998;1:465–70.
39. Wang X, Southard RC, Kilgore MW. The increased expression of peroxisome proliferator-activated receptor- γ 1 in human breast cancer is mediated by selective promoter usage. *Cancer Res* 2004;64:5592–6.
40. Pignatelli M, Cocco C, Santos A, Perez-Castillo A. Enhancement of BRCA1 gene expression by the peroxisome proliferator-activated receptor γ in the MCF-7 breast cancer cell line. *Oncogene* 2003;22:5446–50.
41. Chintharlapalli S, Papineni S, Konopleva M, et al. 2-cyano-3,12-dioxoolean-1,9-dien-28-oic acid (CDDO) and related esters inhibit growth of colon cancer cells through peroxisome proliferator-activated receptor γ -dependent and -independent pathways. *Mol Pharmacol* 2005;68:119–28.
42. Dickson C, Fantl V, Gillett C, et al. Amplification of chromosome band 11q13 and a role for cyclin D1 in human breast cancer. *Cancer Lett* 1995;90:43–50.
43. McIntosh GG, Anderson JJ, Milton I, et al. Determination of the prognostic value of cyclin D1 overexpression in breast cancer. *Oncogene* 1995;11:885–91.
44. Yu Q, Geng Y, Sicinski P. Specific protection against breast cancers by cyclin D1 ablation. *Nature* 2001;411:1017–21.
45. Lee RJ, Albanese C, Fu M, et al. Cyclin D1 is required for transformation by activated Neu and is induced through an E2F-dependent signaling pathway. *Mol Cell Biol* 2000;20:672–83.
46. Wang C, Fu M, D'Amico M, et al. Inhibition of cellular proliferation through I κ B kinase-independent and peroxisome proliferator-activated receptor γ -dependent repression of cyclin D1. *Mol Cell Biol* 2001;21:3057–70.

47. Qin C, Burghardt R, Smith R, et al. Peroxisome proliferator-activated receptor γ agonists induce proteasome-dependent degradation of cyclin D1 and estrogen receptor α in MCF-7 breast cancer cells. *Cancer Res* 2003;63:958–64.
48. Campo PA, Das S, Hsiang CH, et al. Translational regulation of cyclin D1 by 15-deoxy- $\Delta(12,14)$ -prostaglandin J(2). *Cell Growth Differ* 2002;13:409–20.
49. Clay CE, Monjabez A, Thorburn J, Chilton FH, High KP. 15-Deoxy- $\Delta(12,14)$ -prostaglandin J2-induced apoptosis does not require PPAR γ in breast cancer cells. *J Lipid Res* 2002;43:1818–28.
50. Lee SW, Reimer CL, Oh P, Campbell DB, Schnitzer JE. Tumor cell growth inhibition by caveolin re-expression in human breast cancer cells. *Oncogene* 1998;16:1391–7.
51. Li S, Couet J, Lisanti MP. Src tyrosine kinases, G α subunits, and H-Ras share a common membrane-anchored scaffolding protein, caveolin. Caveolin binding negatively regulates the auto-activation of Src tyrosine kinases. *J Biol Chem* 1996;271:29182–90.
52. Couet J, Sargiacomo M, Lisanti MP. Interaction of a receptor tyrosine kinase, EGF-R, with caveolins. Caveolin binding negatively regulates tyrosine and serine/threonine kinase activities. *J Biol Chem* 1997;272:30429–38.
53. Ju H, Zou R, Venema VJ, Venema RC. Direct interaction of endothelial nitric-oxide synthase and caveolin-1 inhibits synthase activity. *J Biol Chem* 1997;272:18522–5.
54. Hulit J, Bash T, Fu M, et al. The cyclin D1 gene is transcriptionally repressed by caveolin-1. *J Biol Chem* 2000;275:21203–9.
55. Mehta RG, Williamson E, Patel MK, Koeffler HP. A ligand of peroxisome proliferator-activated receptor γ , retinoids, and prevention of preneoplastic mammary lesions. *J Natl Cancer Inst* 2000;92:418–23.
56. Stoll BA. Linkage between retinoid and fatty acid receptors: implications for breast cancer prevention. *Eur J Cancer Prev* 2002;11:319–25.
57. Suh N, Wang Y, Williams CR, et al. A new ligand for the peroxisome proliferator-activated receptor- γ (PPAR- γ), GW7845, inhibits rat mammary carcinogenesis. *Cancer Res* 1999;59:5671–3.
58. Noker PE, Gorman GS, Schweikart KM, et al. Pharmacokinetics and toxicity of CDDO, a synthetic triterpenoid, in rats and dogs. *Proc Am Assoc Cancer Res* 2004;45:Abstract 2044.

Molecular Cancer Therapeutics

Synthetic triterpenoid 2-cyano-3,12-dioxoleana-1,9-dien-28-oic acid induces growth arrest in HER2-overexpressing breast cancer cells

Marina Konopleva, Weiguo Zhang, Yue-Xi Shi, et al.

Mol Cancer Ther 2006;5:317-328.

Updated version Access the most recent version of this article at:
<http://mct.aacrjournals.org/content/5/2/317>

Cited articles This article cites 57 articles, 35 of which you can access for free at:
<http://mct.aacrjournals.org/content/5/2/317.full#ref-list-1>

Citing articles This article has been cited by 14 HighWire-hosted articles. Access the articles at:
<http://mct.aacrjournals.org/content/5/2/317.full#related-urls>

E-mail alerts [Sign up to receive free email-alerts](#) related to this article or journal.

Reprints and Subscriptions To order reprints of this article or to subscribe to the journal, contact the AACR Publications Department at pubs@aacr.org.

Permissions To request permission to re-use all or part of this article, use this link
<http://mct.aacrjournals.org/content/5/2/317>.
Click on "Request Permissions" which will take you to the Copyright Clearance Center's (CCC) Rightslink site.